Journal of Nepal Geological Society, 2023, Vol. 66, pp. 119–130
https://doi.org/10.3126/jngs.v66i01.57957

Flood hazard modelling using HEC-RAS in the Pathariya Khola, Far-western Nepal

Bala Ram Upadhyaya[1], Ananta Prasad Gajurel[2,*], Prem Bahadur Thapa[2], Roshan Raj Bhattarai[3], and Megh Raj Dhital[2]

[1]Water Resources Research and Development Centre, Government of Nepal, Lalitpur, Nepal
[2]Department of Geology, Tri-Chandra Multiple Campus, Tribhuvan University, Kathmandu, Nepal
[3]Center for Earthquake Research and Information (CERI), the University of Memphis, USA
**Corresponding author's email: apgajurel@fulbrightmail.org*

ABSTRACT

Flood hazards are a common problem in flat-lying areas, particularly in southern Nepal due to heavy precipitation and the consequent large transportation of sediments from hilly regions. Bank erosion, flooding, inundation, and sedimentation are the major problems in the plain area of the Kailali District along the riverbanks of Pathariya Khola, which is located on the southern flanks of the Churia Range. The study has been focused on flood hazards and vulnerability evaluation. The river discharge was calculated by WECS/DHM method and flood frequency in various return periods was analysed using HEC-RAS, RAS-Mapper, and geographic information system (GIS) for hazard modelling to delineate the flood-prone areas. The flood hazard zones were categorized as moderate (26.29%), high (39.59%), and very high (34.12%) based on the computed water depths of peak floods. The agricultural land is the most vulnerable to flooding followed by built-up areas. The results have revealed that the flood hazard areas are ever-expanding with the increased discharge levels of different return periods.

Keywords*:* River discharge, flood hazard, vulnerability, HEC-RAS modelling, far-western Nepal

Received: 26 April 2023 **Accepted:** 08 July 2023

INTRODUCTION

The uneven distribution of rainfall in mountainous regions of Nepal is a main factor in variable sediment yields and a high drainage density of 0.3 km/km^2 indicates the drainage channels that are vulnerable to flooding events (Shankar, 1985). Flooding in Nepal is further aggravated due to improper land use planning and unauthorized settlements that have resulted in a huge economic loss every year (Sharma et al., 2019). Some researchers carried out the flood hazard assessment around the present study site in Kailali District. From November 2007 to April 2009, Mercy Crops Nepal and the Nepal Red Cross Society Kailali District (NRCS, Kailali) conducted a study on disaster risk that assisted communities in preparing for and responding to floods in the six communities located along the Mohana River and its tributaries in the Kailali District. The potential for flood hazards at larger and smaller scales has been examined in studies using 1D or 2D hydrodynamic modelling techniques (Baky et al., 2019; Beffa, 1998; Cook and Merwade, 2009; Damayanti, 2011; Mani et al., 2014; Vojteková et al., 2015; Werner, 2001), and HEC-RAS has been used to map and evaluate hazards (Karki et. al, 2011; Khanal et al., 2007; Dangol, 2014; Aryal et al., 2020). These studies provide primarily maps of flood inundation for analyses of flood hazards and susceptibility. A hydraulic model and a geographic information system (GIS) were used by Awal et al. (2007) to study the floodplain and map of risk in the Lakhandei River. To evaluate the flood hazard, susceptibility, and risk Masood and Takeuchi (2012) used HEC-RAS and GIS. Flood hazard mapping plays a fundamental role in understanding and managing flood risks, which have been increasing due to urbanization, climate change, and other factors (IPCC, 2014; Kellermann et al., 2020). Flood vulnerability mapping is also an essential aspect related to flood risk assessment and management to provide an understanding of flood risk by identifying areas at risk of flooding and assessing the potential impacts (Abdelkareem and Mansour, 2023).

An important aspect of flood hazard modelling is to acquire geographically distributed data on inundation patterns such as water depth and flow velocity (Kim et al., 2014). Thus, the current work has focused on the issues of comprehending bank failures and modelling flood hazard scenarios in terms of various return periods in Pathariya Khola (river) of Kailali District, far-western Nepal. Moreover, it was intended to encompass the flood hazard zonation that has demarcated the distinct zones of vulnerable areas to flooding as its significance for identifying the degree of vulnerability which is vital for risk reduction strategies (Gallopin, 2006).

GEOMORPHOLOGICAL AND GEOLOGICAL SETTINGS

The watershed of the Pathariya Khola is bounded by latitudes 28˚15'00" and 28˚27'30" N and longitudes 81˚00'00" and 81˚07'30" E (Fig. 1). The study area covers 30 sq.km and the land cover is mainly dominated by agriculture, followed by settlements and forests. The highest rainfall recorded during the monsoon is 1450 mm (DHM, 2022).

Geomorphology

Geomorphologically, the study area comprises the plains and mountainous regions. The southern portion is a gently sloping plain toward the south, whereas the northern portion is mountainous hills. The elevation in the area ranges from 139 m to 1548 m above mean sea level and major tributaries of the Pathariya Khola are Charaila Khola, Rora Khola, and Bijulia Khola.

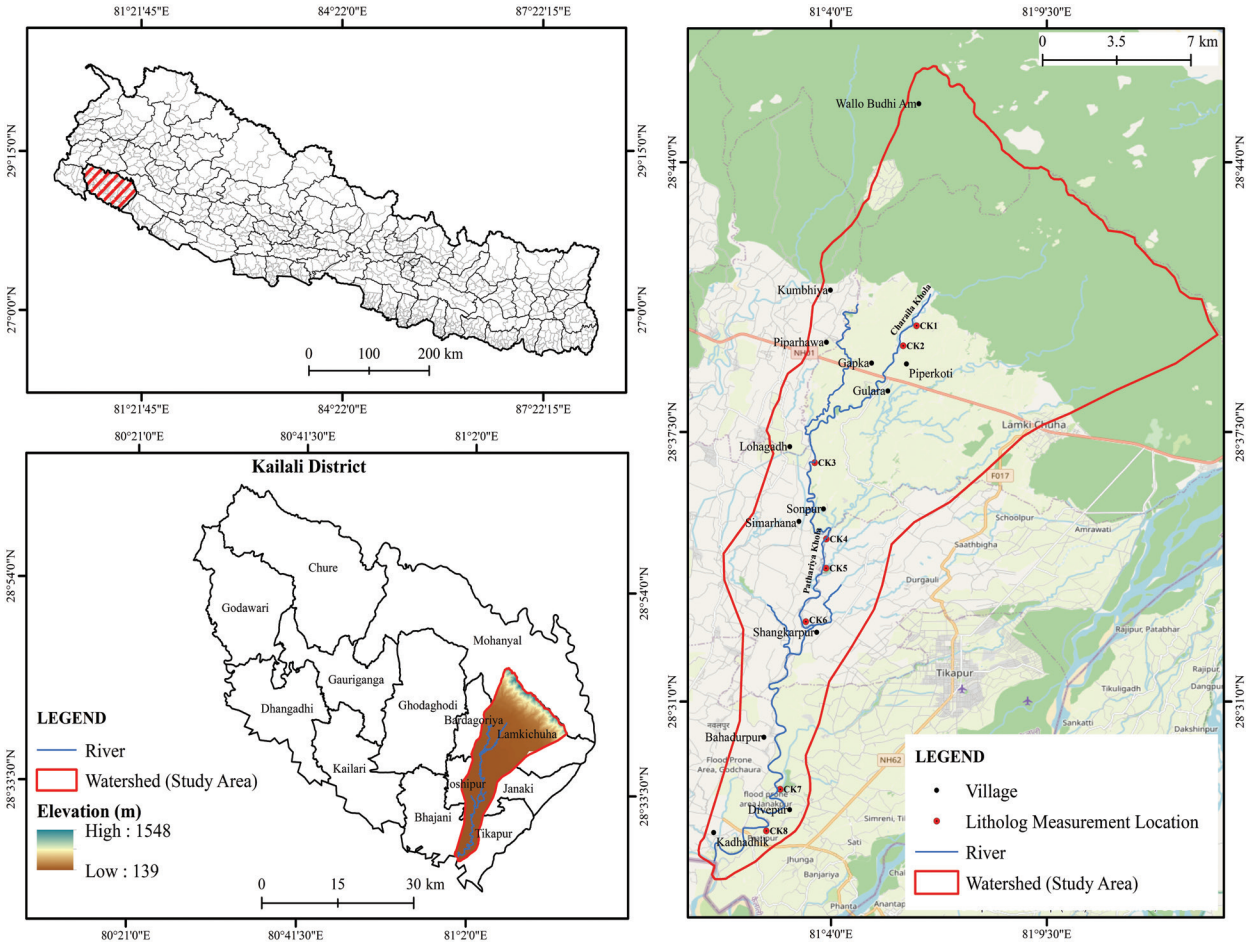

Fig. 1: Location map of the study area.

River morphology: Due to high gradient of Pathariya Khola in the upper reaches of mountainous region, the river transports downstream a significant amount of sediment loads consisting of blocks as well as bounders and pebble-sized clasts. Mid-channel bars are developed in the upper reaches of the Charaila Khola, a tributary of the Pathariya Khola close to Piperkoti village. The river morphology exhibits mainly the meandering channel pattern (Fig. 2a) with high sinuosity whereas the transverse river profile is characterized by a narrow V-shaped in the active channel (Fig. 2b) to asymmetric and U-shaped channel geometry.

River shifting: Geomorphological evidence in the plain areas shows the occurrence of river channel migration. A number of oxbow lakes have formed particularly in downstream areas. River bank erosion and bank failures are significant in the plain area. The channel of Pathariya Khola has been migrating laterally as a result of bank cutting and failures. The superimposition of the river course has indicated the river channel is shifting laterally up to a maximum of 50 m (Fig. 3).

***Riverbank failure*:** Significant issues with the Pathariya River have been known including toe erosion, riverbank cracking, and slumping. Circular bank failures were observed close to Piperkoti village (Fig. 4). In addition to toe-cutting, the force of subsurface water pressure could also accelerate the river bank failures.

Geology

The geology of the study area is divided into sedimentary rocks of the middle Miocene Epoch and semi-consolidated sediments of the Quaternary period (Gautam and Fujiwara, 2000). The sedimentary rocks of the Siwalik (Churia Range) characterize in northern part of the study area (Fig. 5) with northerly dipping sandstone, siltstone, and mudstone (Huyghe et al., 2005). Quaternary geology of the area in southern part comprises the Bhabar Zone, Marshy Land, and Flat Land (Sah et al., 2000). The Bhabar Zone consists of coarse-grained detritus materials ranging in size from boulders to sands. The Marshy Land comprises detrital sediments ranging in size from clay to fine sand. Lithological descriptions of the riverbank materials of Pathariya Khola and its tributaries can be revealed from lithologs. The litholog at river-bank location CK4 is comprised of fine sand at the bottom and light brown silt at the top, whereas clay at the bottom and silt at the top comprises the riverbank at the CK6 (Fig. 6a,b).

DISCHARGE CALCULATION

Discharge calculation is a major component in HEC-RAS modelling for flood hazard evaluation. There are direct and indirect methods for calculating the discharge in hydrological analysis. In the direct method, river flow is based on measured data at gauged river stations and the indirect method uses very few available data or no data near the study area of the un-

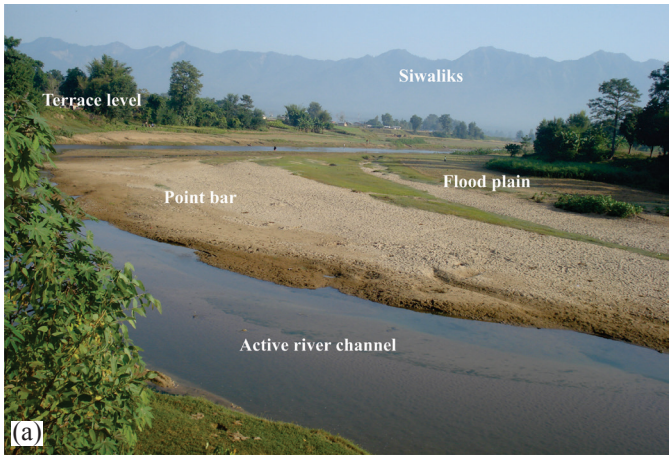

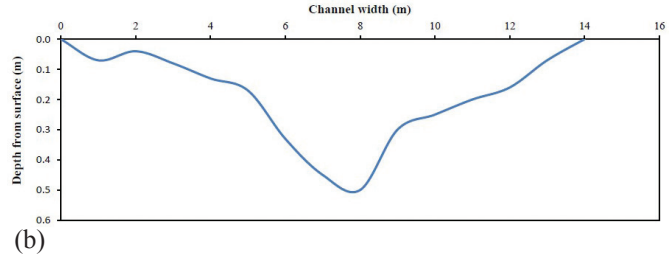

Fig. 2: River morphology of Charaila Khola, a tributary of Pathariya Khola (a) Meandering pattern, (b) typical cross section.

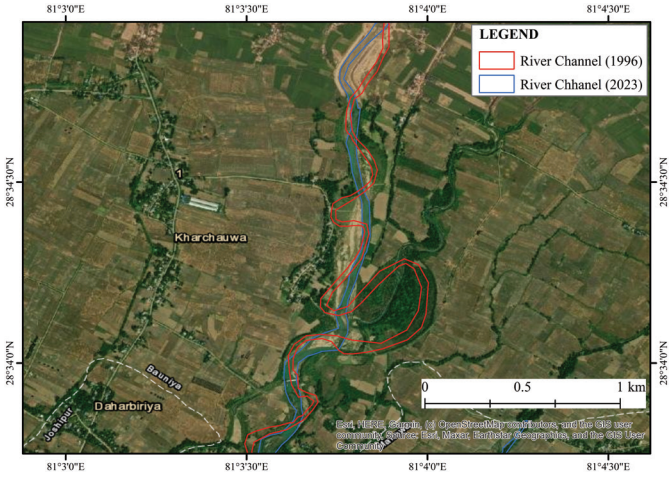

Fig. 3: Lateral shifting of Pathariya Khola from 1996 to 2023.

Fig. 4: Riverbank failure at Piperkoti village of Charaila Khola.

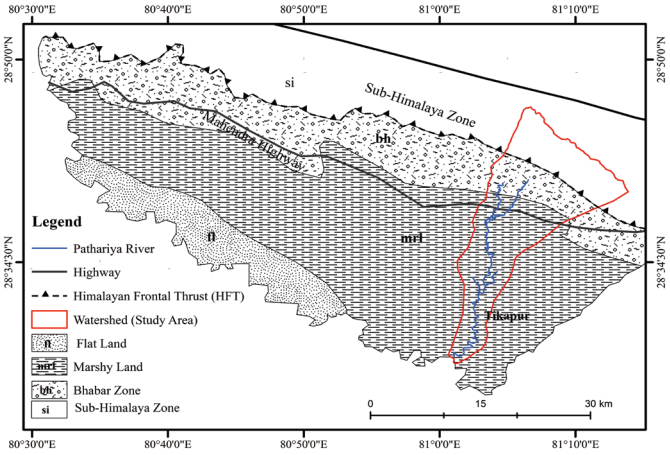

Fig. 5: Generalized geological map of Kailali District (modified after Sah et al., 2006).

gauged catchment. Since the Pathariya Khola and its tributaries lack gauging station, thus, the indirect method was used in the present study to calculate the discharge which includes MHSP, WECS/DHM and modified HYDEST.

Medium Hydropower Study Project Method (MHSP)

The Nepal Electricity Authority created the Medium Hydropower Study Project Method (MHSP) in 1997 and used regional regression techniques to estimate the mean monthly flow for an ungauged site estimate flood flows in a region at ungauged sites. The regression Equation 1 for the flood magnitude and drainage area is as follows:

$$Q = K^{*}Ab \quad (1)$$

where, K and b are regression coefficients that depend on the return period T. A = Drainage area in km^2, Q = Flow in m^3/s

WECS/DHM Method

The Water and Energy Commission and Secretariat (WECS) and DHM collaborated with the World Meteorological Organization (WMO) and the WECS/NEA Institutional Support Programme to establish the WECS/DHM approach in 1990 to estimate the long-term mean monthly flow at an ungauged site (WECS/DHM, 1990). This approach applied for the 2-year and 100-year river's flood flow in catchment area A km^2, which is located below 3000 m, is given in equations (2 and 3).

$$Q_2 = 1.8767\,(A + 1)^{0.8783} \quad (2)$$

$$Q_{100} = 14.63\,(A + 1)^{0.7342} \quad (3)$$

Modified HYDEST Method

The WECS/DHM method has been updated by Sharma and Adhikari (2004) employing a wider range and more hydro-meteorological data in the Modified HYDEST method. For the drainage area lying below 3 km elevation, the flood values for two and one hundred years of return periods (Q_2 and Q_{100}) are determined as shown in equations 4 and 5.

$$Q_2 = 2.29 \times A_{<3km}^{0.86} \quad (4)$$

$$Q_{100} = 20.7 \times A_{<3km}^{0.72} \quad (5)$$

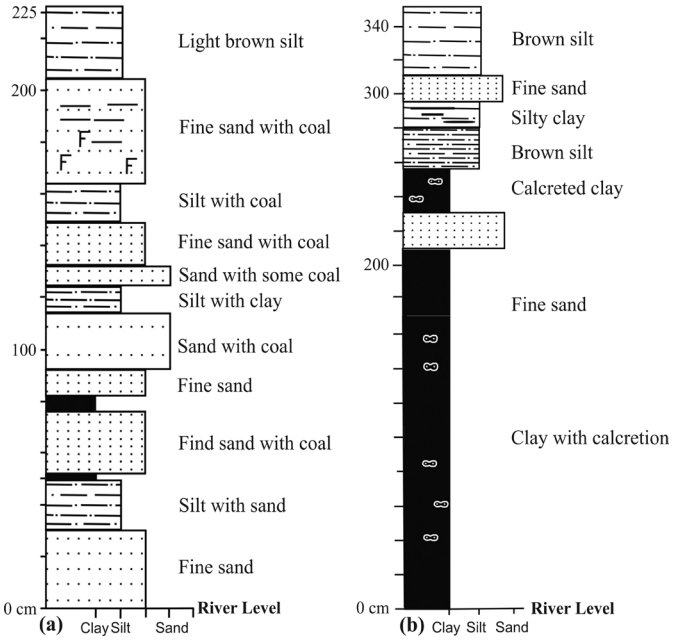

Fig. 6: Representative lithologs along riverbanks of Pathariya Khola (a) CK4 at Sonpur, (b) CK6 at Shangkarpur (See Figure 1 for locations of litholog).

where, Q is the flood discharge in m^3/s and A is the basin area in km^2. The subscript 2 and 100 indicate 2-year and 100-year floods, respectively. Similarly, the subscript < 3 km indicates a catchment area below 3000 m elevation.

According to WECS and DHM (1990), floods in 5, 10, 20, 50 and 200 years return periods are estimated using the following relationship (Eq. 6).

$$QT = \exp(\ln Q_2 + s\sigma) \quad (6)$$

where, A = catchment area below 3000 m elevation

σ = standard deviation of natural logarithms of annual floods = $\ln(Q_{100}/Q_2)/2.326$

s = Standardized normal variants for particular return periods i.e. 0, 0.842, 1.282, 1.645, 2.054, 2.326, and 2.576 for T = 2, 5, 10, 20, 50, 100, and 200 years, respectively.

Maximum flood discharge

The WECS/DHM, Modified HYDEST, and MHSP methods were applied to calculate the maximum flood discharges of 10,000, 1000, 200, 100, 50, 20, 10, 5, and 2 years of return periods for the streams in the model area (Table 1, 2, 3). The volume of discharge increased along with the return period, which is typical of a natural occurrence. The flood estimates for various return periods given by the MHSP method showed higher values compared to the other methods. For the detailed runoff modelling and subsequent flood frequency analysis, the WECS/DHM equation is adopted.

HEC-RAS MODELLING

The Hydrologic Engineering Center's River Analysis System (HEC-RAS) software is widely utilized for hydraulic modeling in flood hazard assessments (HEC-RAS User's Manual, 2020). Due to its accessibility and potential for two-way format conversion between the model and GIS, 1D model is chosen for the present study. HEC-RAS modelling techniques integrated into geographic information systems (GIS) are very effective (Kourgialas and Karatzas, 2011).

Modelling database

Digital Elevation Model (DEM) is the basic input parameter for HEC-RAS modelling. River geometry was created on a reach-by-reach from DEM and imported into the network editor as a shapefile to generate the main river and associated branch tributaries. Each reach is comprised of the river and reach names. The left and right banks as well as the centerlines for rivers were digitized. Flow path centerlines were traced out for all rivers considering both left and right banks, channel flow direction and flow paths. Cross-section lines were generated across the flow of the Pathariya Khola and its tributaries making it perpendicular to the flow direction of river (Fig. 7). Finally, RAS Import file was prepared to generate the geometry and topology in HEC-RAS. Furthermore, Manning's roughness value (n) was assigned with reference to Manning's value provided by Chow (1959). Manning's values for the flood study are assigned to 0.035 for the channel and 0.04 for both the left and right banks of Pathariya Khola and its tributaries. All the geometric data that developed in RAS Mapper were exported to HEC-RAS to compute flood depths for 20, 50, 100, and 200 years of return periods. The processing of the flood simulation in HEC-RAS was performed by using steady flow simulation. In this process, the boundary conditions were established at all the ends of the river nodes by inputting the normal depth. Then, the calculations of water levels, velocities, and inundation extents for different flood scenarios were based on the specified boundary conditions and geometry. The simulated results were used to identify the impacts of floods at varying magnitudes of discharge. A flowchart of processes involved in using HEC-RAS modelling is given in Figure 8.

Modelling results

A series of outcomes were computed and a typical illustration of the generated longitudinal profile of the river for different return periods of inundations in HEC-RAS is shown in Figure 9. Flood areas for return periods of 20, 50, 100, and 200 were 22.33 km^2, 23.43 km^2, 24.54 km^2, and 25.64 km^2 respectively. The highest water depth for the Q_{200} flood scenario is 4.36 m, most of which lies in the stream channel. The water depth for

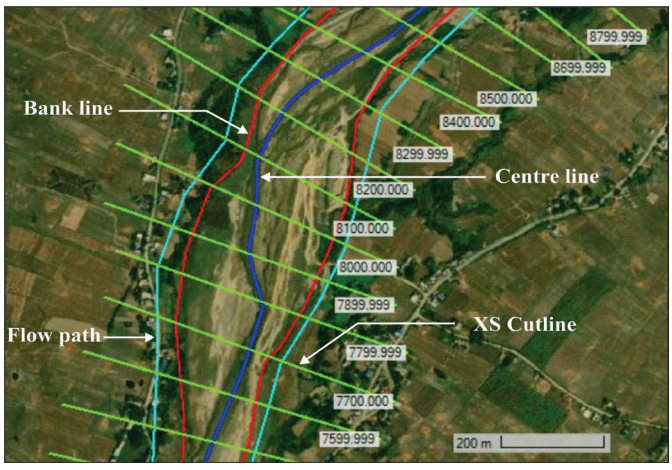

Fig. 7: Channel geometry and topology setup in RAS-Mapper.

Table 1: Flood frequency analysis of the Pathariya Khola.

Return Periods	Calculated discharge (m^3/s)				MHSP	Value Adopted
	WECS/DHM		Modified HYDEST method			
	Daily	Instantaneous	Daily	Instantaneous		
2	106.66	166.91	106.66	171.02		106.66
5	157.33	269.31	157.33	294.28	166	157.33
10	192.77	345.80	192.77	390.80		192.77
20	227.93	425.01	227.93	493.83	251	227.93
50	275.30	536.19	275.30	642.81	314	275.30
100	312.13	625.80	312.13	766.01	368	312.13
200	350.31	721.31	350.31	899.96		350.31

Table 2: Flood estimates of tributaries of the Pathariya Khola by WECS/DHM method.

River	Reach	Discharge (m^3/s) for different return periods (T, year)						
		2	5	10	20	50	100	200
Charaila Khola		37.75	58.10	72.29	87.66	108.09	124.25	141.22
Pathariya Khola	Upper	20.16	31.85	40.44	49.24	61.48	71.26	81.62
Pathariya Khola	Middle 1	68.08	102.28	126.53	150.80	183.78	209.61	236.54
Bijulia Khola		34.53	53.34	66.95	80.76	99.76	114.81	130.63
Pathariya Khola	Middle 2	98.95	146.41	179.67	212.73	257.32	292.04	328.06
Bauniya Khola		11.44	18.50	23.77	29.24	36.92	43.12	49.73
Pathariya Khola	Lower	106.66	157.33	192.77	227.93	275.30	312.13	350.31

Table 3: Flood estimates of tributaries of the Pathariya Khola by MHSP method.

River	Reach	Discharge (m^3/s) with return periods (T, year)					
		5	20	50	100	1000	10000
Charaila Khola		65	100	126	148	242	366
Pathariya Khola	Upper	36	56	71	84	139	212
Pathariya Khola	Middle1	112	170	213	251	403	607
Bijulia Khola		60	92	116	137	224	339
Pathariya Khola	Middle2	157	238	298	349	556	835
Bauniya Khola		15	23	30	36	60	93
Pathariya Khola	Lower	168	254	318	368	586	879

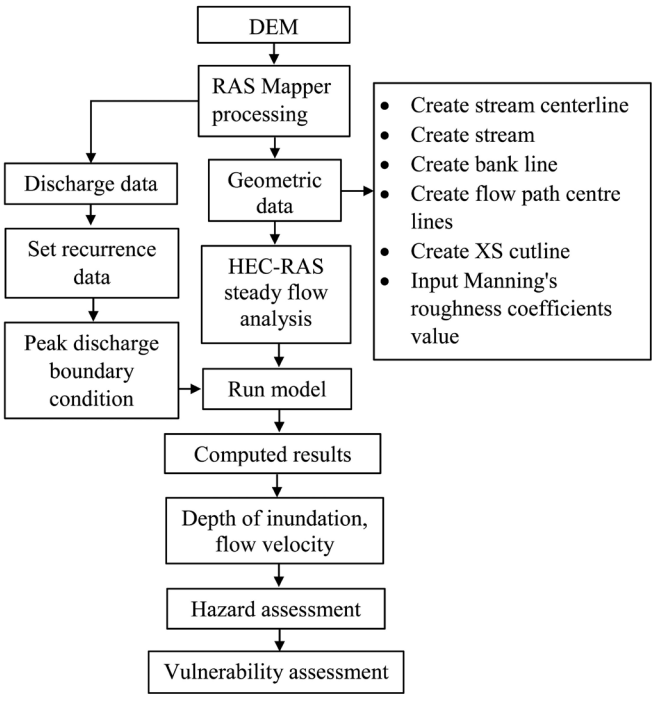

Fig. 8: Flowchart of modelling process in the HEC-RAS.

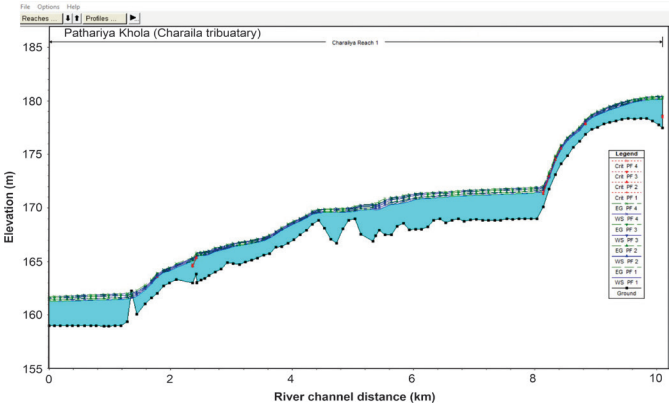

Fig. 9: An illustration of longitudinal river profile for different return periods in HEC-RAS.

the flood scenario of Q_{20} is from 0.001 to 3.82 m (Fig. 10a), whereas it ranges from 0.001 to 3.98 m for the flood discharge of Q_{50} (Fig. 10b), 0.001 to 4.19 m for the flood discharge of Q_{100} (Fig. 10c), and 0.001 to 4.36 m for the flood discharge of Q_{200} (Fig. 10d). Comparison of the simulated floodwater depths of the different return periods indicated that flood characteristics have not changed significantly. In terms of flow velocity, flood discharges were calculated for return periods of 20, 50, 100, and 200 years which are shown in Figures 11a,b,c,d. The lowest

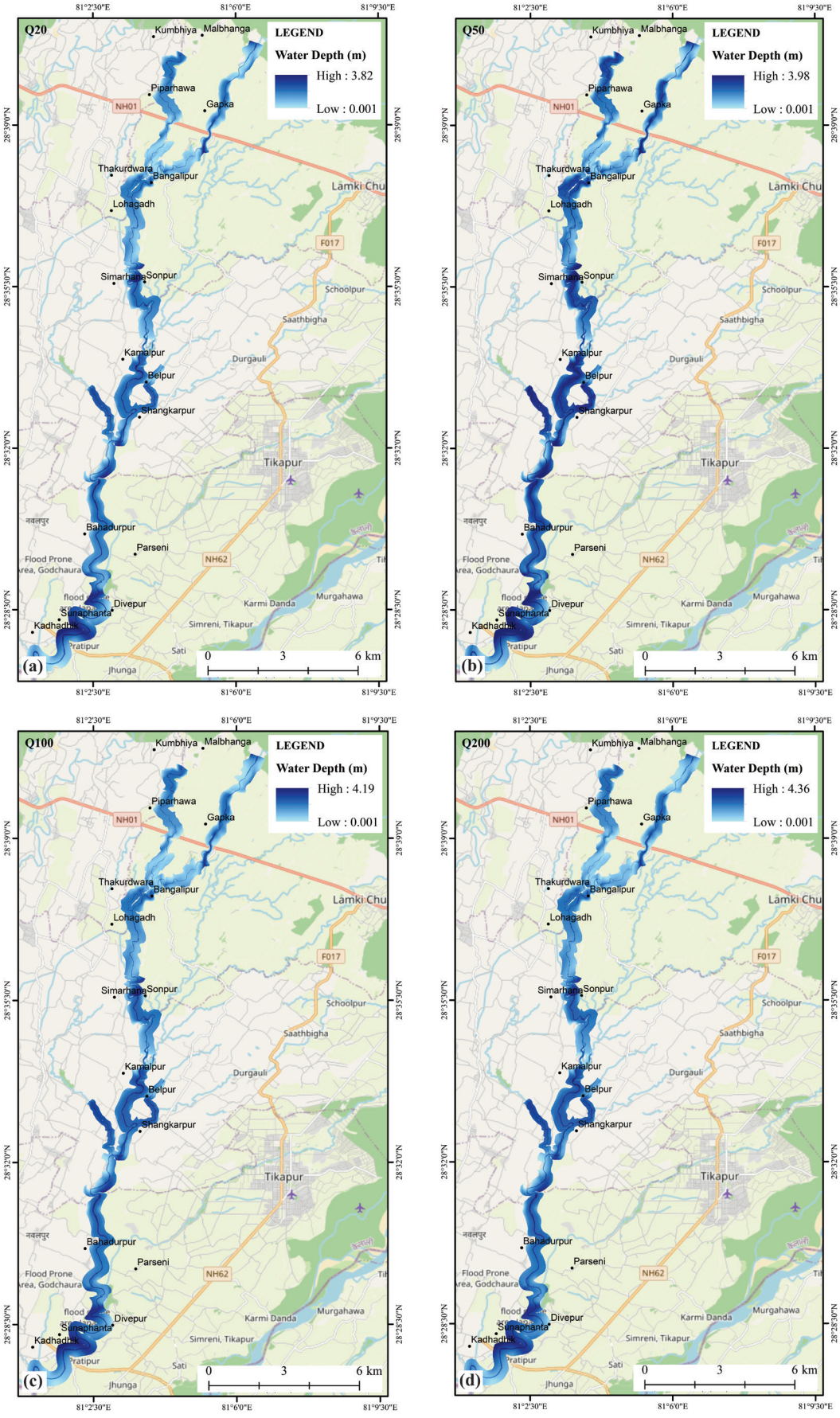

Fig. 10: Water depth in the study area for the flood scenario (a) Q_{20}, (b) Q_{50}, (c) Q_{100}, (d) Q_{200}.

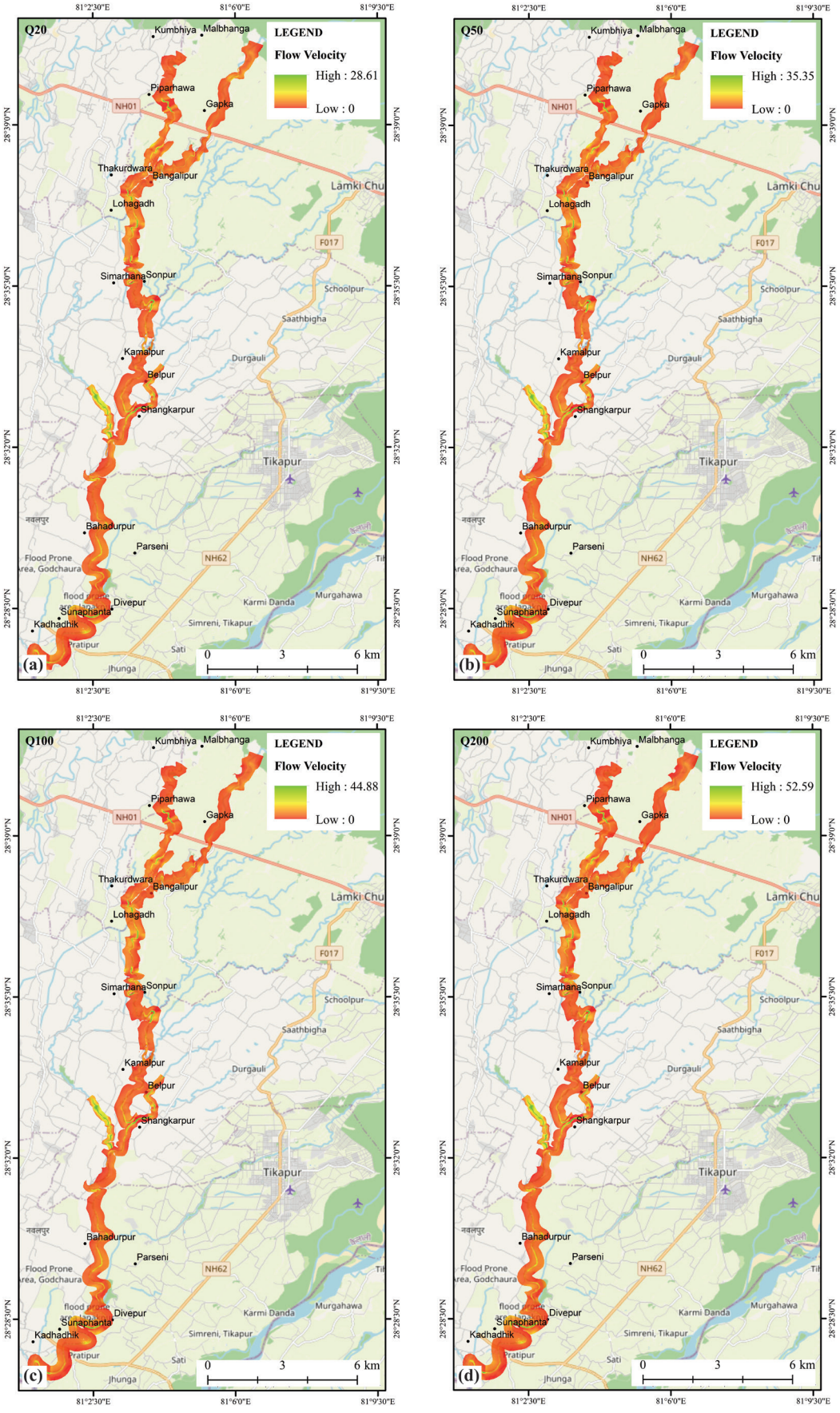

Fig. 11: Flow velocity in the study area for the flood scenario (a) Q_{20}, (b) Q_{50}, (c) Q_{100}, (d) Q_{200}.

velocity is found in Q_{20} which is 28.61 m/s and the highest up to 52.59 m/s for the flood discharge of Q_{200}.

Hazard zonation: The hazard levels were reclassified based on the flood grid and flood depth polygons bounding the water depths. Classification of hazard level categories adopted in this study is based on field conditions and reference values used by other researchers (e.g. MLIT, 2005). The flood plain is categorized as a moderate hazard at a water depth of <0.8 m, a high hazard at a water depth of 0.8–1.6 m, and a very high hazard at a water depth of >1.6 m. In moderate hazards, adult people will not drown and can be evacuated normally. In high hazards, flooding may drown children and adults consequently evacuation becomes difficult (MLIT, 2005). Thus, flood inundation area was classified as moderate, high, and very high. Flood hazard probability for the 20-year, 50-year, 100-year, and 200-year return periods was computed (Fig. 12) and the modelling results are summarized in Table 4. The classified flood depth area indicated that 64% to 73% of the total flooded area has water depths greater than 1.6 m. For the 20-year flood, it is found that the flooded areas with water depths <0.8 m, 0.8–1.6 m, and >1.6 are 8.05 km^2 (36.05%), 11.18 km^2 (50.06%), and 3.1 km^2 (13.88%), respectively, and the 200-year flood covers 6.74 km^2 (26.29%), 10.15 km^2 (39.59%) and 8.75 km^2 (34.12%). The results have shown that flood water depth >1.6 increases the intensity of flooding, and flood water depth <0.8 decreases even with the increasing intensity of flooding.

Vulnerability analysis: Flood vulnerability helps to understand the vulnerability of elements within an area and the land use features of the areas subject to flooding have an impact on flood susceptibility (Gilard, 1996). For vulnerability evaluation, the predicted hazard maps of different outcomes were overlaid/crossed with the land cover map to generate vulnerability maps. A significant part of agricultural land is in a high-risk area. In a 20-year flood, 15.23 km^2 of agricultural land is located in a high-hazard zone, while in a 200-year flood, 17.70 km^2 of the area lies in a high-hazard zone (Table 5). The probabilities of flood vulnerability for different flooding scenarios are given in Figure 13 and Table 6.

DISCUSSION

This study has adopted a hydrological flood model and procedures to estimate the propagation of floods, assess the vulnerable areas of floods, and get a map of areas inundated by flooding at specific discharge values to predict potential flood hazard zones. Application of river flow modelling and GIS for floodplain analyses adopted in this research has been already used for the assessment of hydrological hazards by other researchers where field validation has been established (e.g. Vojtek and Vojteková, 2015; Werner, 2001). Discharge calculation is crucial in the flood hazard modelling that depends on the availability of measurement at gauging station or calculation from the watershed area from the DEM. The unavailability of gauging stations for the studied river puts the work under considerable limitations since one-time measurement of discharge data and its extrapolation for the rest of the time certainly seek detailed measured data for the best result. However, because of wide data usage in the development of WECS/DHM method for flood return period calculation in various periods (Khanal et al., 2007; Dhital, et al., 2010; Karki, et al., 2011; Dangol et al., 2014), the method produced a better representative data set for detailed runoff modelling and flood frequency analysis of various return periods of the study area. While generating water levels for the river discharge, the adopted methodology has focused on flood hazard zonation by extracting cross-sections precisely for modelling the hydraulic characteristics and delineating the floodplain areas. Inundation depth and flow velocity of high flood conditions were calculated by HEC-RAS model to generate the flood hazard categories

Table 4: Probability of flood hazards in various return periods.

Hazard level	20-years		50-years		100-years		200 years	
	Area (km^2)	%	Area (km^2)	%	Area (km^2)	%	Area (km^2)	%
Moderate (<0.8 m)	8.05	36.05	7.75	33.07	7.05	28.73	6.74	26.29
High (0.8–1.6 m)	11.18	50.06	11.30	48.22	10.54	42.95	10.15	39.59
Very High (>1.6 m)	3.1	13.88	4.38	18.69	6.95	28.32	8.75	34.12

Table 5: Flood hazards and vulnerable area in terms of return period.

Category	Total vulnerable area (km^2)							
	20 years		50 years		100 years		200 years	
	Area	%	Area	%	Area	%	Area	%
Agricultural land	15.23	68.32	16.10	68.73	16.91	68.90	17.700	68.93
Built up	2.39	10.72	2.60	11.10	2.9	11.82	3.220	12.54
Bushland	0.190	0.85	0.19	0.81	0.19	0.77	0.190	0.74
Forest	0.075	0.34	0.085	0.36	0.086	0.35	0.090	0.35
Grassland	0.750	3.36	0.76	3.24	0.77	3.14	0.770	3.00
Orchard	0.059	0.26	0.058	0.25	0.058	0.24	0.058	0.23
Pond	0.003	0.01	0.035	0.15	0.0037	0.02	0.004	0.01
River channel	1.820	8.16	1.82	7.77	1.82	7.42	1.840	7.16
Sand	1.770	7.94	1.77	7.56	1.80	7.33	1.800	7.01
Swamp	0.005	0.02	0.0056	0.02	0.0056	0.02	0.0057	0.02

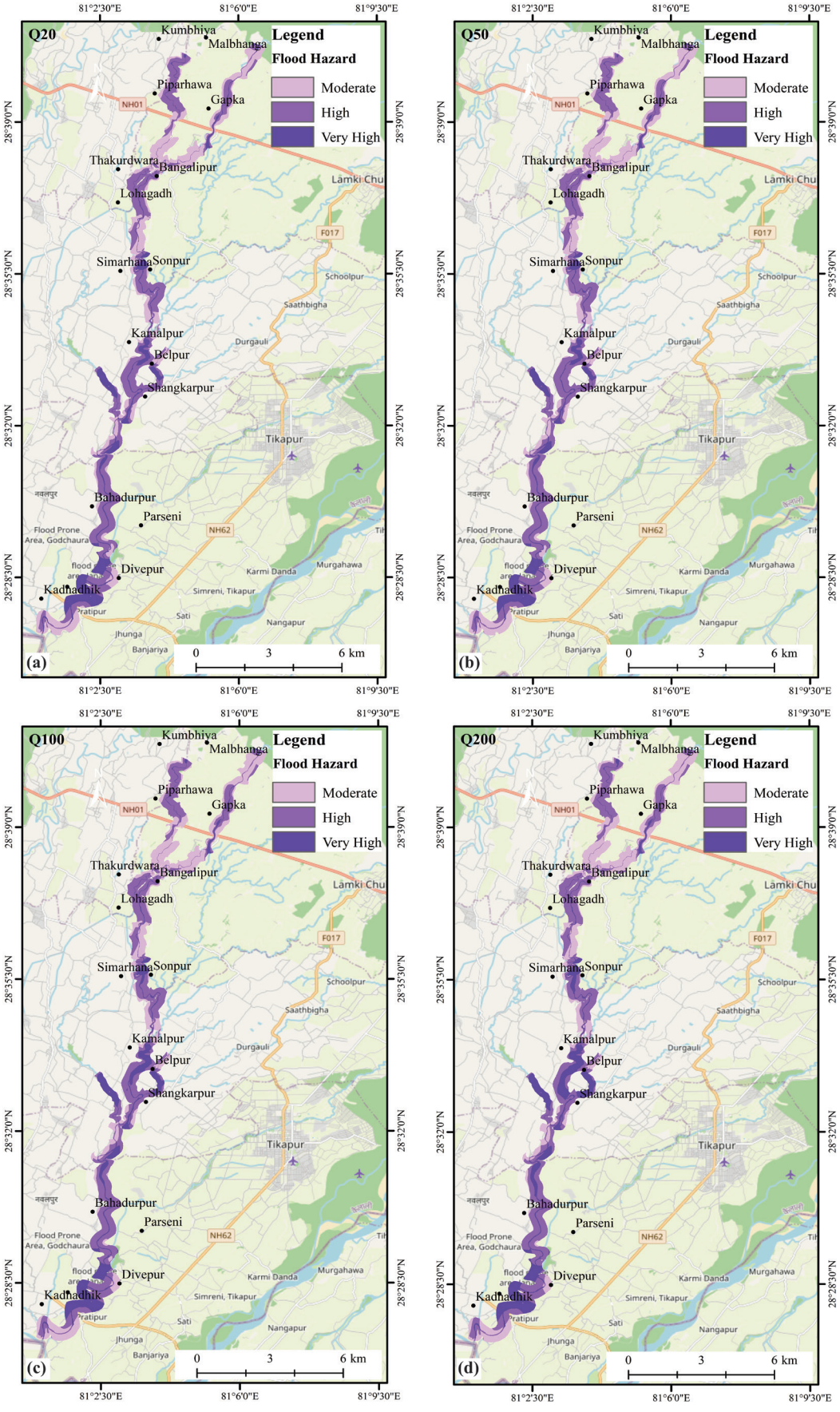

Fig. 12: Flood hazard probability of Pathariya Khola in different return periods (a) 20 years, (b) 50 years, (c) 100 years, (d) 200 years.

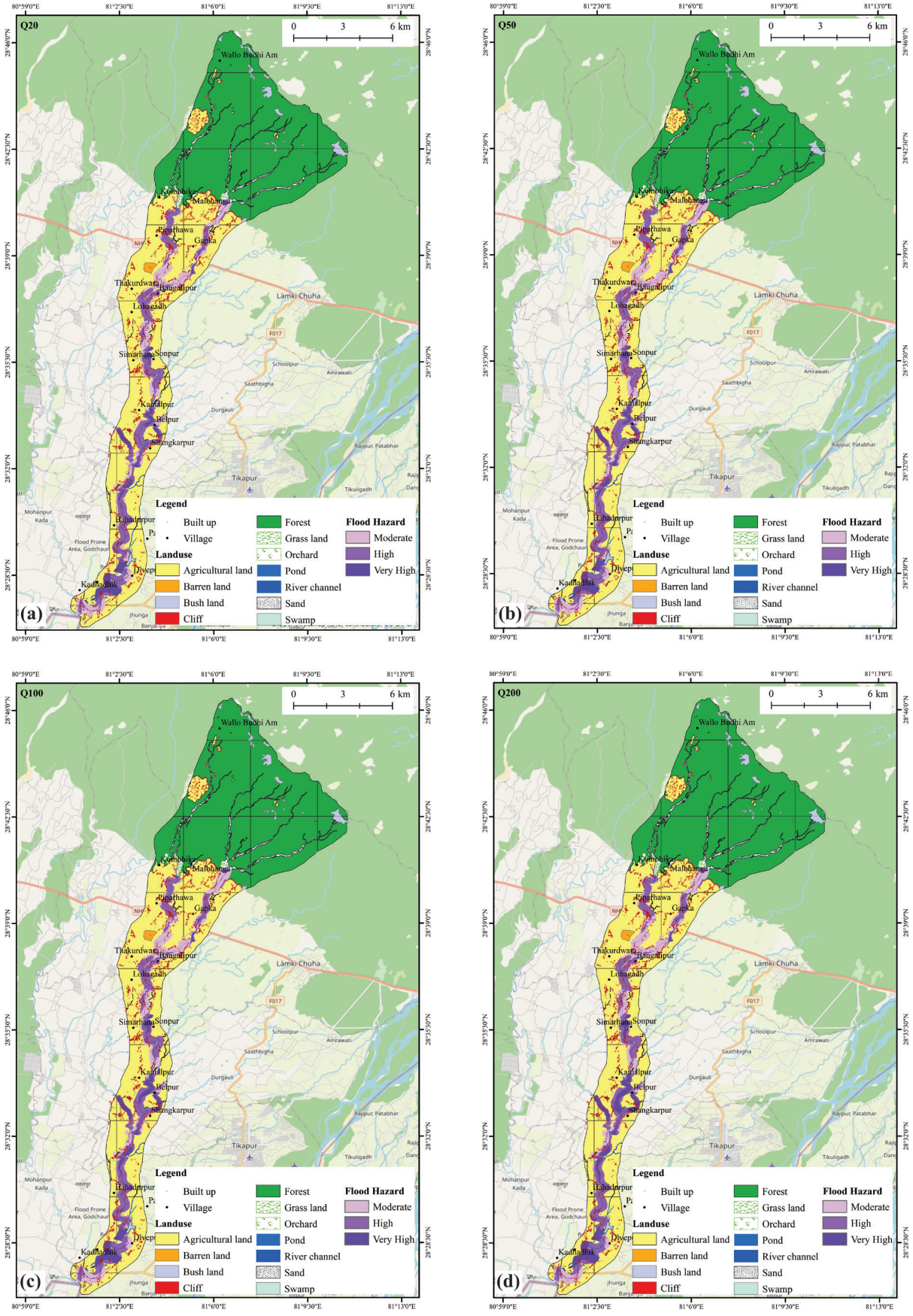

Fig. 13: Flood vulnerability of Pathariya Khola in different return periods (a) 20 years, (b) 50 years, (c) 100 years, (d) 200 years.

Table 6: Flooded area according to land cover with respect to hazard levels.

Land cover	Flood depth (m) and hazard levels	Area (km^2) with return period (years)			
		20 years	50 years	100 years	200 years
Agricultural land	<0.8 m (Moderate)	5.540	5.280	3.950	3.200
	0.8–1.6 (High)	8.030	8.520	8.470	8.220
	>1.6 (Very high)	1.870	2.300	4.750	6.280
Built up	<0.8 m (Moderate)	1.045	1.060	1.200	1.360
	0.8–1.6 (High)	0.690	0.850	0.900	0.970
	>1.6 (Very high)	0.570	0.700	0.800	0.890
Bushland	<0.8 m (Moderate)	0.043	0.004	0.026	0.001
	0.8–1.6 (High)	0.059	0.056	0.046	0.051
	>1.6 (Very high)	0.089	0.100	0.120	0.130
Forest	<0.8 m (Moderate)	0.005	0.007	0.046	0.047
	0.8–1.6 (High)	0.005	0.005	0.006	0.005
	>1.6 (Very high)	0.044	0.180	0.006	0.006
Grassland	<0.8 m(Moderate)	0.240	0.360	0.140	0.130
	0.8–1.6 (High)	0.350	0.190	0.350	0.330
	>1.6 (Very high)	0.140	0.760	0.250	0.280
Orchard	<0.8 m (Moderate)	0.006	0.042	0.003	0.002
	0.8–1.6 (High)	0.042	0.003	0.003	0.002
	>1.6 (Very high)	0.009	0.012	0.024	00.03
Pond	<0.8 m (Moderate)	0.000	0.000	0.000	0.011
	0.8–1.6 (High)	0.003	0.004	0.001	0.000
	>1.6 (Very high)	0.000	0.000	0.002	0.001
River channel	<0.8 m (Moderate)	0.360	0.300	0.240	0.190
	0.8–1.6 (High)	0.910	0.800	0.630	0.550
	>1.6 (Very high)	0.520	0.700	0.940	1.070
Sand	<0.8 m (Moderate)	0.530	0.860	0.380	0.330
	0.8–1.6 (High)	0.300	0.210	0.650	0.560
	>1.6 (Very high)	0.900	0.420	0.720	0.950
Swamp	<0.8 m (Moderate)	0.005	0.005	0.003	0.002
	0.8–1.6 (High)	0.001	0.001	0.002	0.003
	>1.6 (Very high)	0.000	0.000	0.000	0.000

(moderate, high, very high) and were further elaborated in the vulnerability map. The vulnerability analysis of the study has shown that the most vulnerable areas manifest frequent bank failure events and weak geological conditions. Discussions with local people in both villages revealed that the most recent floods that caused serious damage occurred in 1992, 2000, and 2008. During these years, about 15 households were displaced by floods, and they still are living in shelters. A comparison between the flood of the 20-year return period and the 200-year return period showed that flood characteristics have not changed significantly. However, the damaging effect of floods has considerably increased with their regular occurrence in recent years. The assessment of the flooding areas has indicated that agricultural land, which has a flood depth of more than 1.6 m is very high which is also similar to research carried out by Dhital et al. (2010) in Rupandehi District, west Nepal.

CONCLUSION

Flood frequency analysis has illustrated that flood risk is increasing, and river morphological modification and lateral shifting of rivers are actively advancing in Pathariya Khola and its tributaries. Adaptation of WECS/DHM methodology in combination with using HEC-RAS and GIS to create the database for the hydrological modelling results has shown a better prediction of flooding probability by incorporating field evidence. The classified flood hazard levels (moderate, high, very high) were based on the water depth. For the 20-year flood, it is computed that the flooded areas with water depths <0.8 m, 0.8–1.6 m, and >1.6 are 8.05 km^2 (36.05%), 11.18 km^2 (50.06%), and 3.1 km^2 (13.88%), respectively, and the 200-year flood covers 6.74 km^2 (26.29%), 10.15 km^2 (39.59%) and 8.75 km^2 (34.12%). The evaluation of the flood hazard and vulnerability has found a significant coverage of agricultural land is the most vulnerable to flooding, followed by built-up areas. In a 20-year flooding scenario, 15.23 km^2 of agricultural land lies in a high-hazard zone, while in a 200-year flood, 17.70 km^2 of the area is found in a high hazard. The modelling techniques of this study can be helpful for managing flood plains in order to limit future losses and their cascading effects.

REFERENCES

Abdelkareem, M. and Mansour, A. M., 2023, Risk assessment and management of vulnerable areas to flash flood hazards in arid regions using remote sensing and GIS-based knowledge-driven techniques. Nat. Hazards, 117, pp. 2269–2295.

Aryal, D., Wang, L., Adhikari, T. R., Zhou, J., Li, X., Shrestha, M., and Chen, D., 2020, A model-based flood hazard mapping on

the southern slope of Himalaya. Water, 12(2): 540. https://doi.org/10.3390/w12020540.

Awal, R., 2007, Floodplain analysis and risk assessment of Lakhandei River. Innovative Initiatives in Disaster Risk Reduction, pp. 119–128.

Baky, M. A. A., Islam, M., and Paul, S., 2019, Flood hazard, vulnerability and risk assessment for different land use classes using a flow model. Earth Syst. Environ., 4(1), pp. 225–244.

Beffa, C., 1998, Two-dimensional modelling of flood hazards in urban areas. In: Kolz, K. P. (Ed.), 3rd International Conference on Hydro science and Engineering; 1998 August 31 September 3; Cottbus/Berlin: Brandenburg University of Technology.

Chow, V. T., 1959, Open Channel Hydraulics. McGraw Hill Inc., Singapore, 680 p.

Cook, A. and Merwade, V., 2009, Effect of topographic data, geometric configuration and modeling approach on flood inundation mapping. Jour. Hydrol., 377(1-2), pp. 131–142.

Damayanti, F., 2011, Hydrodynamic modeling for flood hazard assessment in Telomoyo Catchment, Central Java, Indonesia. MSc Thesis submitted to Gadjah Mada University and Faculty of Geo-Information Science and Earth Observation, University of Twente, ITC Netherlands, 85 p.

Dangol, S., 2014, Use of Geo-Informatics in flood hazard mapping: A case of Balkhu River. Nepalese Journal of Geoinformatics, 13, pp. 52–57.

Dhital, M., Shrestha, Shrestha, R., Ghimire M., Shrestha, G. B., and Tripati, D., 2010, Hydrological hazard mapping in Rupandehi district, west Nepal. Jour. Nepal Geol. Soc., pp. 59–566.

DHM, 2022, Department of Hydrology and Meteorology (DHM), https://www.dhm.gov.np/

Gallopin, G. C., 2006, Linkages between vulnerability, resilience and adaptive capacity. Global Environ. Change, 16(3), pp. 293–303.

Gautam, P. and Fujiwara, Y., 2000, Magnetic polarity stratigraphy of Siwalik Group sediments of Karnali River section in western Nepal. Geoph. Journal Int., v. 142, pp. 812–824.

Gilard, O., 1996, Flood Risk Management: Risk Cartography for Objective Negotiations. Proc., 3rd IHP/IAHS George Kovacs colloquium, UNESCO, Paris.

HEC-RAS User's Manual, 2020, U.S. Army Corps of Engineers Hydrologic Engineering Center. https://www.hec.usace.army.mil.

Huyghe, P., Mugnier, J. L., Gajurel, A. P., and Delcaillau, B., 2005, Sedimentological analysis of the Karnali River section (Siwaliks of Western Nepal): implication for the Upper Miocene evolution of the Himalayan belt and climate. The Island Arc, v. 14, pp. 311–327.

IPCC, 2014, Climate Change 2014: Impacts, Adaptation, and Vulnerability. Part A: Global and Sectoral Aspects. Contribution of Working Group II to the Fifth Assessment Report of the Intergovernmental Panel on Climate Change (IPCC). In: Field, C. B., Barros, V. R., Dokken, D. J., Mach, K. J., Mastrandrea, M. D., Bilir, T. E., Chatterjee, M., Ebi, K. L., Estrada, Y. O., Genova, R. C., Girma, B., Kissel, E. S., Levy, A. N., MacCracken, S., Mastrandrea, P. R., and White, L. L. (eds.), Cambridge University Press, Cambridge, United Kingdom and New York, NY, USA, 1132 p.

Karki, S., Koirala, M., Pradhan, A. M. S., Thapa, S., Shrestha, A., and Bhattarai, M., 2011, GIS-based flood hazard mapping and vulnerability to climate change assessment: A Case Study from Kankai Watershed, Eastern Nepal. Lalitpur: Nepal Climate Change Knowledge Management Center, Nepal Academy of Science and Technology.

Kellermann, P., Opperman, J. J., and Abell, R., 2020, Climate change-induced flow reductions are projected to worsen end-of-century urban flooding. Frontiers in Earth Science, 8, 113.

Khanal, N. R., Shrestha, M., and Ghimire, M., 2007, Preparing for flood disaster: mapping and assessing hazard in the Ratu Watershed, Nepal. Kathmandu: International Centre for Integrated Mountain Development (ICIMOD), 116 p.

Kim, B., Sanders, B. F., Schubert, J. E., and Famiglietti, J. S., 2014, Mesh type tradeoffs in 2D hydrodynamic modeling of flooding with a Godunov-based flow solver. Adv. Water Resour., 68, pp. 42–61.

Kourgialas, N. N. and Karatzas, G. P., 2011, Flood management and a GIS modelling method to assess flood-hazard areas–a case study. Hydrol. Sci. Jour., 56, pp. 212–225.

Manandhar, B., 2010, Flood Plain Analysis and Risk Assessment of Lothar Khola. Pokhara, Nepal, Institute of Forestry, MSc Thesis submitted to Tribhuvan University (unpublished), 65 p.

Mani P., Chatterjee C., and Kumar R., 2014, Flood hazard assessment with multiparameter approach derived from coupled 1D and 2D hydrodynamic flow model. Nat. Hazards, 70(2), pp. 1553–1574.

Masood, M. and Takeuchi, K., 2012, Assessment of flood hazard, vulnerability and risk of mid-eastern Dhaka using DEM and 1D hydrodynamic model. Natural Hazards, v. 61(2), pp. 757–770,

Mercy Crops, 2008, Kailali disaster risk reduction report. Mercy Crops Nepal in partnership with Nepal Red Cross Society Kailali District, 29 p.

MLIT, 2005, Ministry of Land Infrastructures and Transport (MLIT), Flood hazard mapping manual in Japan (Manual RIBAGUA 13 para mapas de riesgos de inundación en Japón). Tokyo: Ministry of Land Infrastructure and Transport, 73 p.

Sah R. B., Shrestha D., and Gorkhali S., 2000, Geology and plant fossil in from the Siwaliks of Godawari area, Sub-Himalaya, Far Western Nepal. Jour. Strat. Assoc. Nepal, v. 2, pp. 42–52.

Shanker, K., 1985, Water Resources. In: Majupuria, T. C. (Ed.), Nepal: Nature's Paradise, White Lotus Co., Bangkok, pp. 25–31.

Sharma, K. P. and Adhikari, N. R., 2004, Hydrological Estimations in Nepal. Department of Hydrology Meteorology, Government of Nepal, Nepal, 104 p.

Sharma, T. P. P., Zhang, J., Koju, U. A., Zhang, S., Bai, Y., and Suwal, M. K., 2019, Review of flood disaster studies in Nepal: A remote sensing perspective. International journal of disaster risk reduction, 34, pp. 18–27.

Vojtek, M. and Vojteková J., 2015, Flood hazard and flood risk assessment at the local spatial scale: a case study. Nat. Hazards, v. 7(6), pp. 1973–1992.

WECS/DHM, 1990, Methodology for Estimating Hydrological Characteristics of Ungauged Locations in Nepal, His Majesty's Government of Nepal. Ministry of Water Resources, Seq. No. 331, Water and Energy Commission Secretariat and Department of Hydrology and Meteorology, (WECS/DHM), Kathmandu.

Werner, M. G. F., 2001, Impact of grid size in GIS based flood extent mapping using 1D flow model. Phys. Chem. Earth., 26, pp. 517–522.